NASA/TM–2019-220245

Reduction of Wind Tunnel Contamination During Flow Visualization Experiments using Polystyrene Microspheres

Russell C. Schmitz and Jan Genzer
North Carolina State University, Raleigh, North Carolina

Pacita I. Tiemsin and Christopher J. Wohl
Langley Research Center, Hampton, Virginia

April 2019

NASA STI Program . . . in Profile

Since its founding, NASA has been dedicated to the advancement of aeronautics and space science. The NASA scientific and technical information (STI) program plays a key part in helping NASA maintain this important role.

The NASA STI program operates under the auspices of the Agency Chief Information Officer. It collects, organizes, provides for archiving, and disseminates NASA's STI. The NASA STI program provides access to the NTRS Registered and its public interface, the NASA Technical Reports Server, thus providing one of the largest collections of aeronautical and space science STI in the world. Results are published in both non-NASA channels and by NASA in the NASA STI Report Series, which includes the following report types:

- TECHNICAL PUBLICATION. Reports of completed research or a major significant phase of research that present the results of NASA Programs and include extensive data or theoretical analysis. Includes compilations of significant scientific and technical data and information deemed to be of continuing reference value. NASA counter-part of peer-reviewed formal professional papers but has less stringent limitations on manuscript length and extent of graphic presentations.

- TECHNICAL MEMORANDUM. Scientific and technical findings that are preliminary or of specialized interest, e.g., quick release reports, working papers, and bibliographies that contain minimal annotation. Does not contain extensive analysis.

- CONTRACTOR REPORT. Scientific and technical findings by NASA-sponsored contractors and grantees.

- CONFERENCE PUBLICATION. Collected papers from scientific and technical conferences, symposia, seminars, or other meetings sponsored or co-sponsored by NASA.

- SPECIAL PUBLICATION. Scientific, technical, or historical information from NASA programs, projects, and missions, often concerned with subjects having substantial public interest.

- TECHNICAL TRANSLATION. English-language translations of foreign scientific and technical material pertinent to NASA's mission.

Specialized services also include organizing and publishing research results, distributing specialized research announcements and feeds, providing information desk and personal search support, and enabling data exchange services.

For more information about the NASA STI program, see the following:

- Access the NASA STI program home page at http://www.sti.nasa.gov

- E-mail your question to help@sti.nasa.gov

- Phone the NASA STI Information Desk at 757-864-9658

- Write to:
  NASA STI Information Desk
  Mail Stop 148
  NASA Langley Research Center
  Hampton, VA 23681-2199

NASA/TM–2019-220245

Reduction of Wind Tunnel Contamination During Flow Visualization Experiments using Polystyrene Microspheres

Russell C. Schmitz and Jan Genzer
North Carolina State University, Raleigh, North Carolina

Pacita I. Tiemsin and Christopher J. Wohl
Langley Research Center, Hampton, Virginia

National Aeronautics and
Space Administration

Langley Research Center
Hampton, Virginia 23681-2199

April 2019

Available from:

NASA STI Program / Mail Stop 148
NASA Langley Research Center
Hampton, VA 23681-2199
Fax: 757-864-6500

Abstract

Evaluation of novel methods and materials for seeding tracer particles for particle image velocimetry (PIV) was carried out in the Basic Aerodynamic Research Tunnel (BART) at NASA's Langley Research Center (LaRC). Seeding of polystyrene latex microspheres (PSLs) from ethanol/water suspensions and from the dry state was carried out using custom built seeders. PIV data generated using the novel methods were found to be in general agreement with data collected using the current seeding methods. Techniques for assessing PSL fouling of wind tunnel surfaces were identified and refined. Initial results suggest that dry seeding PSLs may allow comparable data quality to wet seeding while reducing wind tunnel screen fouling. Results also indicate that further developments to the dry seeding system should focus on increasing single particle flux into the wind tunnel. Modifications to PSLs and seeding equipment to achieve this have been identified and are discussed.

Introduction

Wind tunnel studies are employed to investigate the aerodynamics of structures moving through a medium (e.g., a plane through the atmosphere) at a length scale which allows precise control and measurement of system variables. In most wind tunnel experiments, the structure being studied is stationary while the medium moves around it (e.g., a model airplane in front of a fan). Particle image velocimetry (PIV) is a method for characterizing the movement of the medium in wind tunnel studies. In PIV, tracer particles are injected into the moving medium and tracked using high-speed photography to generate 2D and 3D vector maps of fluid movement. The amount and quality of data that may be collected depends on tracer particle properties, including size, size distribution, shape, density and refractive index. NASA researchers have investigated polystyrene latex microspheres (PSLs) as a promising tracer material since the 1980s[1]. One limitation regarding the use of PSLs in wind tunnel experiments is that PSLs adhere to exposed surfaces, particularly the screens that smooth the flow profile of air entering the test section. Concerns about the potential for PSL contamination to affect experimental results and increase facility cleaning costs have prevented wider utilization of PSLs in wind tunnel studies.

Recent efforts to characterize, understand and mitigate surface fouling by PSLs have identified some promising approaches. The conventional method for PSL seeding in wind tunnels involves aerosolizing a suspension of PSLs in a water/alcohol solution through an ultrasonic nozzle. Liquid droplets form on surfaces close to the nozzle as a result of vapor condensation or incomplete droplet evaporation from the aerosol. Testing revealed that the presence of liquid on a surface correlated with increases in both the extent of PSL fouling and difficulty of PSL removal. A systematic study was performed to assess how the presence of solvent influenced PSL surface contamination[2]. Experiments showed that, even with the use of a more volatile solvent composition (e.g., pure ethanol instead of an aqueous ethanol solution), surface contamination by PSLs occurred if any solvent remained at the position of surface contact. The solvent provided a capillary force that increased the overall interaction strength and provided a medium for the PSL to adopt a more stable orientation on the impacted surface leading to even greater interaction strength. This indicates that changes to PSL seeding methods offer a simple way to reduce PSL fouling.

Modification of PSL surfaces offers an alternative route to address PSL fouling. Characterizations of PSL surface properties are available in the literature and demonstrate that PSL surfaces bear anionic groups. One promising PSL modification approach is to associate cationic surfactants with these anionic surface groups. An evaluation of the relationship between surface chemical modification and PSL contamination is ongoing at North Carolina State University (NCSU) and NASA Langley Research Center (LaRC) as part of the same "Clean Screen PSL" investigation that motivated the work described here. Presented in this TM are some preliminary results of this effort.

Recapture of PSLs entrained in flow is desirable to minimize potential PSL contamination in closed-return wind tunnels. An electrostatic particle capture device (EPC) was deployed and tested during wind tunnel tests described here. The design and development of this system is ongoing and will be described in a future document. Briefly, in an EPC device, particles pass through a strong magnetic field between two electrodes and become electrostatically charged. These charged particles are then repelled from the electrodes and collected on the ground plate. A test device was constructed based on literature that was evaluated through the course of the testing described in this report[3].

This Technical Memorandum is divided into four sections. The first section describes preparation, properties and modification of PSLs. The second section covers the theory and design of a fluidized bed for dry seeding PSLs in wind tunnels. The third section describes the tests carried out in the Basic Aerodynamic Research Tunnel (BART) at LaRC using unmodified and modified PSLs with variations of conventional 'wet' seeding methods and dry seeding from a fluidized bed. The goals of these tests are discussed below. The fourth section discusses the lessons learned over the course of this investigation and highlights promising avenues for future work.

Goals:

1) Establish methodologies for quantitative comparisons of PSL fouling in an active research wind tunnel. Operating in an active research facility instead of on a lab bench constrained what samples and measurements could be taken and a discussion of these limitations and efforts to work around them is provided below. These tests provide a proof-of-concept for application of PSLs in active research facilities and they establish a framework for conducting and evaluating future tests. This document is intended to provide a detailed procedure for wind tunnel tests with PSLs and related equipment to streamline and optimize future tests.
2) Compare 'wet' vs. 'dry' seeding techniques and determine if dry seeding techniques do, in fact, result in reduced screen fouling. The design of the 'fluidized bed seeder' (FBS) is discussed alongside the practical details of implementing this design in an active research wind tunnel. The use of fumed silica additives and chemically modified PSLs to improve seeding from the FBS is also evaluated.
3) Evaluate the potential for 'dry' seeding to reach the seed density needed to generate viable data in wind tunnel tests and evaluate the need for increasing seed density from an FBS.

Polystyrene Latex Particles: Synthesis, Properties and Modification

Soap-Free Emulsion Polymerization (SFEP)

Two-phase processes, like emulsion or dispersion polymerization, are often employed to generate polymer microparticles because they offer rapid heat transfer and control of particle morphology without mechanical processing. Microparticles are often made from polystyrene (PS), which has been extensively studied over the last century. The use of surfactants to improve solubility of reactants and products is common in emulsion polymerization, but results in relatively broad particle size distributions and smaller particles[4]. Surfactants also become incorporated into particles and interfaces, further complicating characterization of the process and products. SFEP, which requires no surfactants, is a convenient alternative for creating monodisperse microparticles with controllable size and surface properties[4–7].

This work uses free-radical polymerization of styrene monomer in an aqueous continuous phase to produce PSLs. The steps of polymerization are shown in **Appendix A**. The initiator is water-soluble potassium persulfate (KPS). Magnesium sulfate ($MgSO_4$) is used to control size, as described below. Typical reactant amounts (the "base recipe") are given in **Appendix A**. Styrene monomer is purified by vacuum distillation. Deionized water is deoxygenated by sparging with nitrogen. The reaction is run under a nitrogen blanket and all steps are designed to prevent oxygen entering the system. A reactor is charged with water, monomer, and $MgSO_4$. The reaction mixture is stirred and sparged with nitrogen to remove any remaining oxygen while the temperature is raised to 70°C. After 30 minutes, the sparger is removed and KPS solution is injected into the reactor. 21 hours after KPS injection, the reactor is removed from the heating bath, opened to the air and allowed to cool. The latex product is collected in amber bottles and stored away from light. A discussion of relevant phenomena in SFEP is provided below. Detailed discussions of mechanisms, kinetics and the impact of SFEP conditions on PSL properties are available in the literature[4,6–19].

Mechanisms of SFEP

Upon the injection of KPS, it thermally decomposes to produce free radicals and SFEP proceeds through three intervals, shown in **Appendix A**[6]. Interval I begins with monomer droplets in a continuous phase which is saturated with dissolved monomer. Some free radicals initiate polymerization in monomer droplets (heterogeneous nucleation), but most free radicals react with dissolved monomer, creating solvated oligomeric radicals. The concentration and size of the solvated oligomers increase until they precipitate, forming a large number of particles in less than a second (homogeneous nucleation)[6]. The formation of these particles marks the transition between Intervals

I and II. During Interval II, monomer diffuses out of droplets and enters the growing particles and the aqueous phase remains saturated with monomer. Polymer initiation occurs in the aqueous phase, as well as in particles and droplets. The huge number of particles rapidly capture primary or oligomeric radicals from solution and as a result the particles are the only significant loci of polymer growth[16,17]. Over Interval II, particles grow by swelling with monomer, capturing oligomers from solution, and coalescing with other particles[9]. The depletion of free monomer in the droplets signals the start of Interval III, where the aqueous concentration of monomer decreases, the number and size of particles stabilize, and polymerization eventually stops. SFEP reactions described in this work were typically run for 21 hours.

PSL Properties as a Function of SFEP Conditions

Styrene and PS surfaces are hydrophobic but PSL surfaces are hydrophilic due to the presence of sulfate, hydroxyl, and carboxyl groups. The typical concentration of acid groups on a PSL surface are ~0.5 acid groups per nm^2 [5,20]. Polymerization initiated by a sulfate radical results in a chain with a hydrophilic sulfate end group, and these concentrate at the particle surface[20]. Hydroxyl surface groups may be derived from initiation by a hydroxyl radical (formed from the Kolthoff reaction) or by hydrolysis of an alkyl sulfate. Carboxyl groups originate from the oxidation of hydroxyl groups[6,13,15,21–23]. Therefore, the initiator plays a key role in stabilizing PSLs. In contrast, the initiator increases the ionic strength of the aqueous phase, which has a destabilizing effect. Screening of electrostatic repulsion between charged PSL surfaces increases with ionic strength, thus lowering the barrier to particle aggregation and coalescence. Increased coalescence in Interval II leads to fewer, larger particles[6,9,15,22]. This may also be achieved by the addition of $MgSO_4$, which does not contribute to surface stabilization. Typical values reported for surface charge density, σ, of PSLs from SFEP are between 1 and 10 $\mu C/cm^2$ [5,12,20,23,24]. The final product of SFEP, as described here, is acidic (pH~2-3) due to surface acid groups and sulfuric acid formed in side reactions[6].

Modification of PSLs

Styrene and polystyrene are hydrophobic, but the surfaces of polystyrene latex microparticles synthesized through soap-free emulsion polymerization are hydrophilic. This is due to the presence of acidic sulfate, hydroxyl and carboxyl groups on the particle surface, derived from the potassium persulfate initiator or from side reactions during synthesis. This process has been studied extensively and reported values for the concentration of acid groups on a particle surface are on the order of 0.5 acid groups per nm^2 [5,20]. Association of quaternary alkylammonium (QA) species with surface anions/acids has been reported as a method to decrease the interfacial tension and hydrophilicity of a range of materials[25–28]. The bulky quaternary ammonium head group electrostatically associates with and neutralizes a surface acid, while the hydrophobic alkyl tail can mask other higher-energy surface species.

Functionalized PSLs (fPSLs) were produced by modification of PSLs with QAs to investigate how particle adhesion and fouling might be impacted by changes to the particle surfaces. For this study, the QAs cetyltrimethyl ammonium bromide (CTAB) and didodecyldimethyl ammonium bromide (10-10-DAB) were used. A method for modification of PSLs with QAs was developed based on methods reported in the literature. The most important consideration in this method was to avoid using QA concentrations at or above the critical micelle concentration (CMC), in order to avoid formation of admicelles on PSL surfaces[28,29]. Further investigation into the modification of PSLs with QAs is ongoing and will be described in more detail in a future document.

Pre-Modification Cleaning

Approximately two liters of PSL Batch 030907 were used for modification tests. The particles in suspension were cleaned by centrifugation to remove any solvated or lighter-than-water species such as salts, oligomers and

residual styrene monomer. A Sorvall RC-5B Superspeed Centrifuge equipped with a 3-liter GS-3 rotor was used to spin the samples at 6,000 rpm for 15 minutes. After centrifuging, the PSL samples consisted of a clear supernatant on top of a cake of solids. The supernatant was decanted and replaced with an equal volume of deionized (16 MΩ·cm) water. The cake of solids was broken up and resuspended in this deionized water with a combination of vortex-mixing and ultrasonication. Once the sample appeared homogenous, the centrifuge/decant/resuspend cycle was repeated two additional times.

After cleaning, the centrifuge tubes containing cleaned PSLs were recombined into one container, then divided equally between two flasks. Deionized water was added to each flask to bring the total volume per flask up to 1 L.

Particle Modification

The theoretical maximum number of QAs needed to completely cover a PSL surface was calculated based on a particle diameter (D) of 1 micrometer, a particle concentration of 10% by mass in suspension, and a surface density of 1 QA molecule per 2 nm^2 of PSL surface. This "theoretical maximum" (as opposed to the stoichiometric amount) is an intentionally high estimate to allow for variation in particle size and surface composition between batches (**Appendix B**).

The CMC values from the literature were used for each QA (**Appendix B**)[30]. To minimize the opportunity for micellization to interfere with functionalization, QA was added to each flask in two stages. After the first QA addition, the flasks were sealed and stirred on a hotplate set to 50°C for 24 hours before the second addition. The amount of QA added in each stage is given in Appendix B. After the second addition, the flasks were resealed and stirred for an additional 72 hours. At this point stirring was stopped and the samples were cleaned by centrifugation. The spin/decant/resuspend process described earlier was repeated three times for each sample. After a fourth centrifugation step, the supernatant was poured off and the caked solids transferred to jars for drying. Drying was accomplished by leaving the jars uncapped on a hotplate set at 90°C for 48 hours, at which point the PSLs were visibly dry. Any large chunks were broken up with a spatula and the jars were then transferred to a vacuum oven and dried under vacuum at 70°C for 24 hours. Tests at BART were conducted with both unmodified PSLs (uPSLs) and QA functionalized PSLs (fPSLs).

The Fluidized Bed

Prior investigations indicated that the presence of liquid during PSL seeding increases the extent and strength of PSL fouling of surfaces[2]. Dry seeding of PSLs rigorously dried has been considered as an alternative but poses unique challenges. PSLs are stable in water but are prone to aggregation in the dry state, thus producing a very broad particle size distribution. Seeding of the dry powder requires breaking up of aggregates into single particles, separating single particles from aggregates, mobilization of particles into the air and transportation of airborne particles to the seeding point. We designed a fluidized bed system to address these requirements.

Fluidization Principles

Fluidization is the process of passing a fluid upwards through a bed of solid particles at a high enough velocity that the aerodynamic drag on the particles is comparable to the gravitational forces on the particles. Upon fluidization, the particles are suspended in the fluid and exhibit fluidic behavior (Fig 1). The fluidized particles may be transported as a fluid through tubing, an advantage for transporting particles from the fluidized bed to the seeding point. The fluidized bed also has a viscosity comparable to the fluid used to entrain the particles, *i.e.*, very good mixing can be

achieved in fluidized beds. This was considered advantageous for breaking up PSL aggregates in the bed prior to seeding.

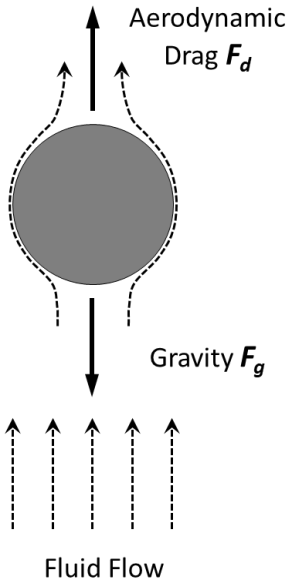

Figure 1. Forces on a particle due to drag and gravity. Particle-particle and particle-wall forces are not shown.

With respect to fluidization of PSLs, the most important considerations are particle density and size. The Geldart classification scheme groups particles into four general categories (A, B, C, D) of fluidization behavior based on particle size and density [31]. PSLs used here fall into group C of Geldart's classification scheme. Group C particles are typified by very strong and difficult to overcome bonds between individual particles. In some applications group C particles are often considered simply too difficult to even attempt to employ in fluidization. This is because as the particle size decreases, the attractive van der Waals force between particles decreases more slowly than the gravitational and hydrodynamic forces on each particle. The result is agglomeration between group C particles with minimal fluidization of individual particles. Many studies have been done to induce fluidization of group C particles, with some success [32–44]. Common techniques include physical agitation of the particles by vibration, acoustic pressure, or mechanical stirring. These methods can improve the quality of fluidization to a limited extent. All have the goal of breaking up channeling and maldistribution of particles in the bed, which occurs when the fluidizing air passes directly through the bed in small tunnels, entraining very little of the particles in the bed. Attempts have also been made to alter the forces themselves that adhere the particles to one another. Methods include coating particles or contacting surfaces in a conducting material or introducing nanoparticles into the bed [45–48].

Fluidization Theory for PSL Seeding

In an ideal fluidized bed, every particle experiences an upward drag force (from the moving fluid) counteracting the downwards force of gravity. When the drag and gravitational forces on every particle are equal, the particles are in a perfect floating suspension and the bed is said to be fully fluidized. The degree of fluidization can be increased past full fluidization by increasing the fluid density or flow rate, indicating that pneumatic convection has begun and particles are now being carried out of the bed [49].

When fluidizing PSLs for wind tunnel seeding, the complexities caused by group C fluidization are not as challenging as might be expected because perfect fluidization is not required. The purpose of the fluidized bed in this work was to allow a controllable number of particles to become entrained in an airflow, so perfect fluidization was not the goal. Therefore, measures to enhance the fluidization of PSLs are not required, *unless the enhancement of fluidization quality also leads to increased controllability of single particle entrainment*. It is suspected that a fully fluidized bed would deliver more individual particles and allow better control than an otherwise identical bed with lower fluidization quality; this remains to be demonstrated.

Fluidized Bed Background

Fluidized beds can be broken down into 4 basic components: particles, suspending fluid, distributor, and fluidization riser (Fig. 2) [31]. Size, shape, density, and electrostatic characteristics of the particles play a role in how

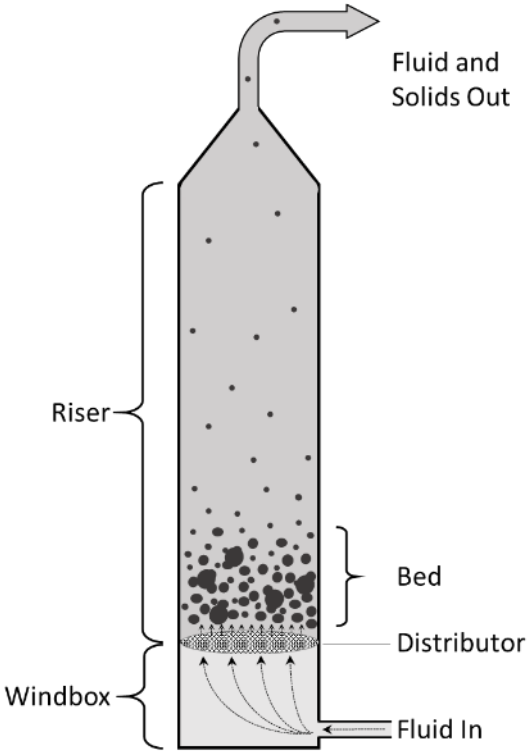

Figure 2. Parts of a fluidized bed.

the particles will fluidize. The Geldart classification scale provides approximate information about how different particles are likely to respond to attempts at fluidization [31].

Suspending fluid denotes the fluid pumped through the particle bed to suspend them against the pull of gravity. This fluid can be either gas or liquid; the most common gas being compressed air and the most common liquid being water. The air distributor is typically a porous plate or filter that allows the suspending fluid to pass evenly into the bed and through the particles. The most important characteristic of the air distributor is that its pores be small enough to not allow the particles to pass through, but large enough to allow suspending fluid through at a rate that allows fluidization. Smaller beds typically use a mesh filter or screen, while larger industrial size beds often use flat plates with evenly spaced holes.

The fluidization riser is the container for the particles. Typically, it is cylindrical, and (for laboratory operations) is made of glass, acrylic, or another transparent material. 2D beds, consisting of two flat plates with a thin film of particles between them, are also occasionally used for lab operations. 2D beds are especially useful for studying the phenomenon of bubbling as it occurs inside the bed [38].

Formation, breakup and retention of PSL agglomerates in the bed are important in determining the single particle to agglomerate ratio (SP:AG) that the bed can elute[48]. The characteristics that make PSLs attractive for PIV flow tracking (uniform geometry and small size) are lost if the seeded particles are in large 20 - 100 μm agglomerates rather than 1 - 2 μm individual particles [50]**.** This makes the ability to elute only the smallest particles in the bed a key requirement of the fluidized bed seeding system.

Another challenge to seeding PSLs stems from the difficulty inherent in characterizing the behavior of the bed over time. Fluidized beds, especially in batch operation like the FBS, are dynamic systems and small variations in operating/ambient conditions, handling, etc. can lead to variations among tests, making reproducibility challenging. As the bed is operating and particles are eluted, the nature of the bed is necessarily changing; the overall mass of particles present is decreasing, the charge of the particles is changing, and agglomerates are being formed and broken up. This leads to difficulty in theoretically predicting how many particles are being delivered into the airflow at a given time. However, this does not mean that large discrepancies should be expected over moderate time scales so long as loading and pressure conditions are similar; It is expected that experiential control of seeding will be adequate for most PIV applications.

Addition of Nanoparticles

Another avenue of study for improving PSL fluidization is the addition of smaller nanoparticles into the mixture [45–48]. Our preliminary investigations indicate that fumed silica nanoparticles are effective for improving fluidization of PSLs, though the exact method of action is unknown. Analysis using scanning electron microscopy (SEM) of PSL/silica mixtures shows that the silica and PSLs do not interact strongly with each other, and that most silica particles form large agglomerates themselves, away from the PSL surfaces. The silica particles have been hypothesized to act as either a lubricant between the PSLs or as a desiccant to encourage further drying of the PSLs, but neither of these has been confirmed[51].

Design of Prototype Fluidized Bed

Design considerations for a prototype dry seeding fluidized bed began with materials. Laboratory scale beds should have a transparent riser to allow visual inspection of fluidization and mobilization of particles within the bed. Static charging between group C particles is a common problem, so a material that minimizes tribocharging of the particles is desired[52–55]. The affinity of a material in the triboelectric series corresponds to its tendency to gain (affinity < 0) or lose (affinity > 0) electrons from tribocharging. The severity of tribocharging becomes smaller the closer two materials are in the triboelectric series. Transparent poly(vinyl chloride) (PVC) was chosen for its proximity to

polystyrene in the triboelectric series and commercial availability (Table 1). As an easily-machinable and inexpensive material, PVC also allowed facile construction and rapid prototyping of the bed.

Table 1. Triboelectric series of selected materials.

Material	Affinity (nC/J)
Polyurethane Foam	+60
Glass	+25
Wool	0
Polymethyl Methacrylate	-10
Polystyrene	-70
Polyvinyl Chloride	-100

The air distributors chosen were Sterlitech 0.6 μm, 90 mm diameter glass fiber filters that could retain single PSLs with a low pressure drop across the filter.

After entrainment in the rising air flow, single particles must be removed from the bed riser and introduced into wind tunnel air flow. Venturi vacuum pumps were utilized for this purpose by creating a controllable pressure drop, pulling particles from the bed to the nozzle without the need to pressurize the FBS. The Venturi vacuum pumps were fitted with brass high-volume clog-resistant full cone spray nozzles to widely disperse particles leaving the nozzle. The ultrasonic atomizing nozzles utilized for traditional wet seeding are not amenable to a gas-only system.

The suction lines of the vacuum pumps were connected to three holes equally spaced around the top of the PVC bed riser via static-dissipative polyurethane tubing. Static-dissipative tubing was chosen to minimize further charging and adhesion of particles between elution and seeding. All connections between the vacuum pumps and bed riser were push-to-connect fittings, with no valves, to prevent obstruction of particle flow. The top of the riser was capped with another glass filter to prevent particles from escaping out of the bed.

Fluidized Bed Construction

The PVC components of the bed were all size 3 schedule 80 PVC pipe. The 61 cm (24 in.) riser was clear PVC pipe, as was the windbox. The windbox was connected to the riser by two flanges and the Sterlitech glass filter air distributor was sandwiched between two polymer meshes clamped between the flanges. Pressure into the bed was controlled via a needle valve and monitored by an analog pressure gauge. The top of the fluidization column was capped off with another glass filter to keep PSLs contained in the column and filter the output air. Having the top of the riser open to the atmosphere also allowed the Venturi pumps to be run without air flow into the bed, because makeup air could enter through the top filter. Three equally spaced holes were drilled 15 cm from the top of the riser and equipped with quick connect airline fittings. These air lines, made up of static dissipative tubing, were vacuum lines running to three individual VP20-100M Vaccon Venturi vacuum pumps. The cone nozzles were mounted on the outlets to the vacuum pumps. The bed was supported on a plywood stand, with the flange bolts also securing the FBS to the stand. A diagram of the prototype bed is shown in Fig. 3.

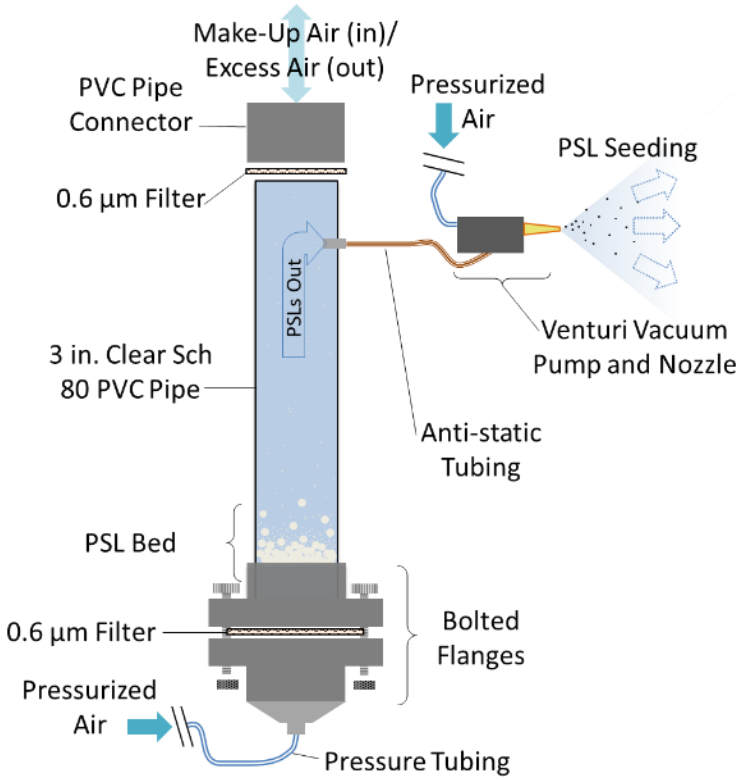

Figure 3. Components of the Fluidized Bed Seeder.

BART Activities

Facility Description

The BART wind tunnel at LaRC is an open-return wind tunnel (Fig. 4) operating at ambient (indoor) temperature and pressure and subsonic velocities. The entire wind tunnel is enclosed in one air-conditioned room. The maximum velocity in the test section is 67 m/sec (220 ft/sec) and air passes through a honeycomb and four anti-turbulence screens before entering the test section. The contraction ratio of the tunnel is 11:1. The steel honeycomb covering the intake of the wind tunnel is four inches thick with a 0.64 cm (1/4 in.) cell size. The honeycomb is 269.2 cm (106 in.) high by 304.8 cm (120 in.) wide. The base of the honeycomb is 30.5 cm (12 in.) above the surface of the floor. Behind the honeycomb, the four screens are 20 mesh per inch with a porosity of 64%. The screens are made from stainless steel and mounted on rails so they may be removed from the wind tunnel for inspection and cleaning.

Screen Preparation

Characterization of wind tunnel screen fouling requires a baseline from which to judge screen cleanliness. For this investigation, only the first screen in the series of 4 screens in BART is considered and all further references

to the screen will be specific to the first screen in the tunnel, directly behind the honeycomb. This screen is chosen because it is assumed that it would be the most fouled of all the wind tunnel screens and initial observations confirmed this assumption.

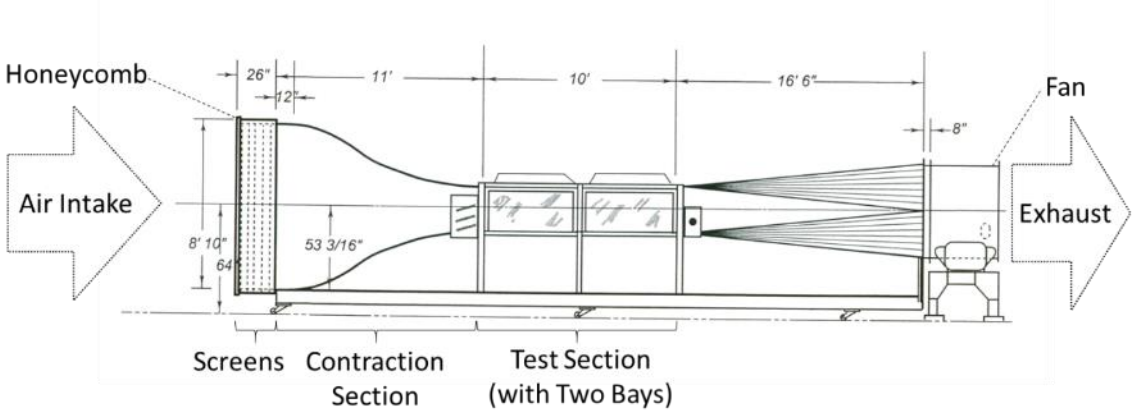

Figure 4. The Basic Aerodynamics Research Tunnel

Before any cleaning was done, the screen was visually inspected to determine its initial state of cleanliness. Areas of interest on the screen were determined based on the location of the PSL seeding nozzles. The areas of interest were those areas immediately downstream of the seeding nozzles and therefore the areas expected to be most affected by fouling. These areas were first cleaned exhaustively using a variety of methods, as described below. Once the 'initial clean' was complete, the screens were cleaned between each round of PSL seeding to return them to the baseline cleanliness. Samples from the screen were collected periodically to confirm the cleanliness of the screen after cleaning procedures.

Initial Observations

Initial visual inspection of the screen revealed that the screen surface was completely covered in a yellowish film, with areas of greater discoloration in the center. The origin of this film is unclear, but it seems reasonable to expect it to be based on a combination of seeding materials used in the tunnel over the years including "Pea Soup" fog liquid and PSLs. These materials could have built up on the screen over time and been chemically altered by oxidation and the use of organic solvents during cleaning. A piece of glassware covered in PSLs may be cleaned with soap and water; however, PSLs can melt and fuse onto a surface if exposed to an organic solvent. Based on the nature of the contaminant present on the screens, it appears that this may have occurred, contributing to the yellowish coating that covered the screen. The cleaning agent "Prep-Sol 3919S™" was used to clean the screens and a primary ingredient of this cleaning agent is hydrotreated heavy naphtha. This is capable of swelling and dissolving PSLs. Therefore, it is possible that some component of the film on the screen was polystyrene from PSLs that had been essentially dissolved and subsequently coated the wires comprising the screen. Samples from the screen revealed no discrete PSLs or monolayers of PSLs, or even material identifiable as derived from PSLs. (Fig. 5).

Visual inspection of the screen revealed areas of higher fouling visible as increased yellowing on the screen. Closer inspection showed the contaminant film to be thicker in these regions. The regions of high fouling seemed to correspond to the areas where seed was injected into the wind tunnel, *i.e.*, directly downstream from where nozzles would be located during seeding.

The initial inspection also identified the presence of numerous indented areas in the screen, typically less than one cm wide and a few mm deep. These indents did not follow a clear spatial pattern; it was assumed that they were the result of foreign object damage from previous tests.

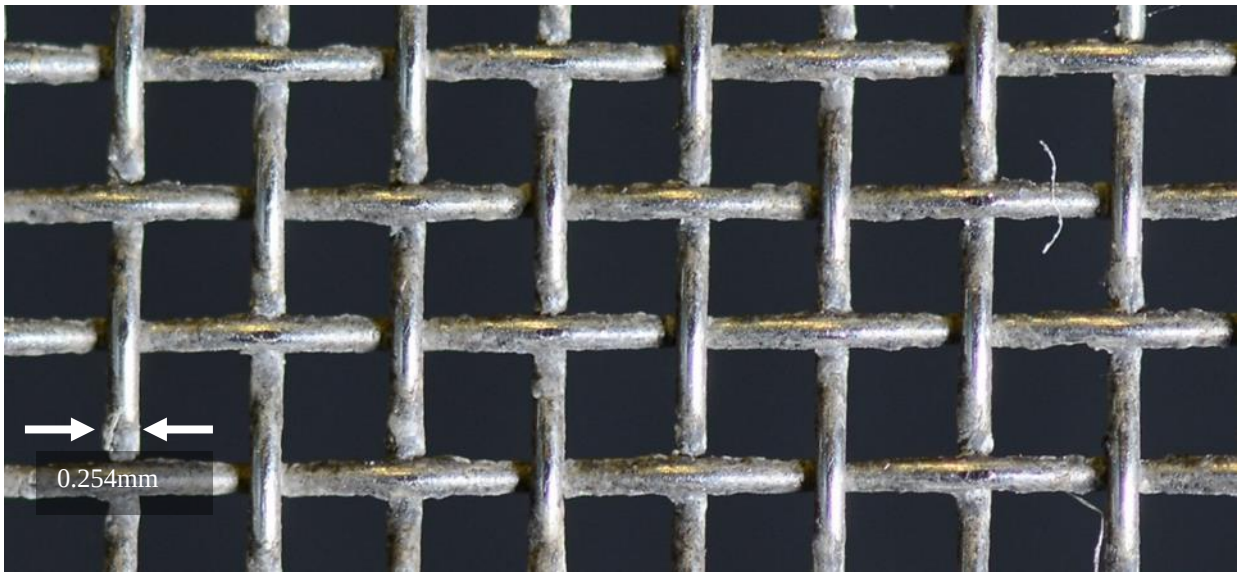

Figure 5. BART screens before cleaning

Initial Cleaning

Various cleaning methods were tested for the initial cleaning of the screen as it was not immediately clear what would most effectively remove the contaminant film. The first method attempted for cleaning the screen was wiping the screen down with the terrycloth steaming attachment of a SHARK® brand commercial clothes steamer. According to facility personnel, this was the conventional cleaning method. The terrycloth/steamer cleaning was found to be completely ineffective at removing the contaminant film, however. The next cleaning method was to wipe the screens down with "Simple Green®" all-purpose cleaner, a solvent-free water-based degreaser. Simple Green was sprayed on a lab wipe which was then employed to wipe the screen. This procedure was also found to be ineffective at removing the contaminant film. The next cleaning method was using "Prep-Sol 3919S" degreaser, which was observed to slightly reduce the contaminant film thickness but did not remove the film to any visible extent. The Prep-Sol also raised concerns about inhalation exposure for prolonged use and the possibility of solvating the PSLs and coating the screen. The final cleaning method employed was gentle brushing with a green plastic scouring pad, using Simple Green to wet the pad. Brushing was carried out by wetting the scouring pad with Simple Green and then placing it gently on the surface of the screen and moving it parallel to the screen. During brushing it was of the utmost importance to minimize pressure on the screen, so that most of the scouring came from the motion parallel to the screen. The most effective brushing method was found to be folding a 8 cm x 8 cm square of scouring pad in half, holding the folded pad by the overlapping edges to make a loop with the material, and brushing the loop back and forth across the surface of the screen. The contaminant film flaked off during brushing, rather than dissolving. The

amount of contaminant on the screen can be seen from the pile of flakes that dislodged from the screen (Fig. 6). Only the front of the screen was cleaned.

Figure 6. Flakes of contaminant removed from screen during cleaning. Lab wipes (approximately 30 cm x 30cm each) positioned below screen to facilitate clean-up.

After brushing, the screens were cleaned by wiping with the terrycloth pad attached to the steamer. The steamer was filled with cold tap water and no additives were used. In the past cleaning had been carried out using a commercial cleaning additive to the water in the steamer. Both sides of the screen were cleaned with the steamer. The screen was left out of its slot for at least an hour after steaming to allow it to dry completely.

As an interesting anecdote, previous screen cleaning methods contrast with the care taken to protect the screen during the current investigation. According to facility personnel, the old-fashioned way to clean the screens was to lay them flat in the parking lot and hose them down while scrubbing with a push-broom.

Cleaning Between Fouling Tests

After each seeding test, samples were collected from the wind tunnel screen and then the screen was cleaned before the next round of testing. The cleaning between tests consisted of wiping down both sides of the screen with

the terrycloth pad attached to the SHARK steamer. Visual and photographic inspection of the screens confirmed that this cleaning was sufficient to remove any particles that were deposited on the screen, and that no film had formed on the screen during testing or cleaning. In some places on the screen, the initial contaminant film persisted and the steamer was ineffective at removing these patches. The efficacy of particle removal with the steamer was confirmed by contact paper samples collected from the screens at various times during testing and cleaning.

Data Collection Methods

Operating Conditions

Data and observations on operating conditions during testing were collected with the aid of a standardized form that was filled out for each testing run, to ensure uniform record-keeping. The form (**APPENDIX C**) documented the type of seeding (wet or dry), additives to the PSL seed, locations of seeding nozzles and pressures within the system (supply pressure, pressure to the seeding nozzles and pressure to the seeding vessel). Operating conditions for the test were recorded, including seeding start/stop times, tunnel air speed and observations.

Screen Fouling

Photographs

Photographs of the screen were taken at various times during testing using a Nikon D800 camera with a macro zoom lens at maximum magnification. External illumination for photographs was provided by a LED lamp (F&R Standard 5600k Flood K400) that was held at various distances and angles to the substrate to provide the greatest contrast. The camera was mounted on a tripod and a 10 s timer was used to allow vibrations from handling the camera to dissipate before capturing an image. Individual particles could not be resolved in the photographs but aggregates could be detected and the color and texture of the wire surfaces was visibly different at different levels of PSL contamination.

Photographs of the wind tunnel screen were taken before and after the initial cleaning, and then after each wind tunnel test. Photographs were taken before any samples were collected from the screen, and after the first several rounds of cleaning to confirm that the cleaning procedure was adequately removing PSLs. To provide a uniform backdrop, a black cloth was hung behind the screen before photographing. Photographs were taken at various locations on the screen during initial cleaning and testing to adequately characterize the whole screen and capture any salient features. Between wind tunnel tests, photographs were taken at the point of the screen directly in front of the seeding nozzles. The exact location of photographs was tracked by measuring the horizontal distance to the right-hand-side edge of the screen and the height of the tripod.

Dicing Tape

Dicing tape (Semiconductor Equipment Corporation, Blue Low Tack Roll P/N 18733) was used to sample selected areas of the screen for particulate contamination. Dicing tape comprises a polymer film backing coated on one side with a low-tack adhesive. Dicing tape was chosen because it is soft and flexible and designed to leave no residue on surfaces when removed. When pressed onto the wind tunnel screen the dicing tape follows the contours of the screen, pushing the adhesive into interstitial spaces. When the tape is removed from the screen PSLS are transferred from the screen onto the tape. The tape was examined under a microscope to characterize PSL coverage on the screens.

A sampling mount was constructed to hold the dicing tape and improve uniformity of the sampling procedure. The sampling mount (Fig. 7) consisted of a 15.2 cm x 3.8 cm x 8.9 cm (6 in. x 1.5 in. x 3.5 in.) length of wood with a

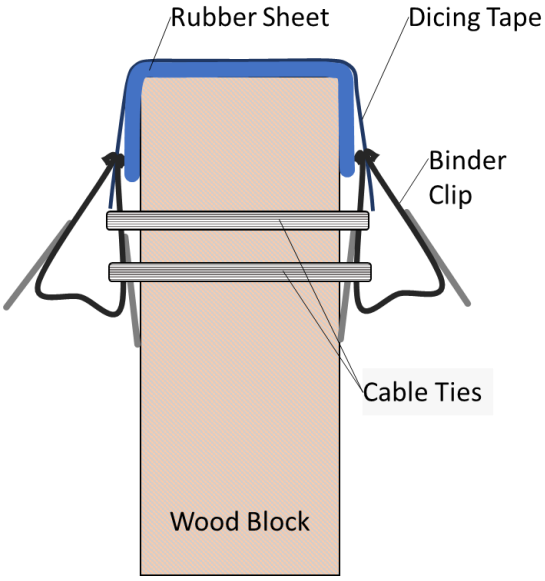

Figure 7. Mount for collecting dicing tape samples.

rubber sheet stretched over one end. Binder clips for holding a piece of dicing tape were secured to either side using cable ties. The rubber mat provided a deformable surface to improve the contact between dicing tape and wind tunnel screen. To collect a sample, a 10 cm x 8 cm piece of dicing tape was clipped onto the mount using the binder clips. One researcher pressed the mount (with dicing tape) onto the front of the screen with a rolling motion while a second researcher used a clean gloved hand to support the back of the screen. This procedure ensured good contact between the dicing tape and the screen while protecting the screen from any deformation. After pressing the sampling mount against the screen, the dicing tape sample was unclipped from the mount, then trimmed into a 5 cm x 5 cm square centered on the area of contact with the screen. Trimmed samples were stored adhesive side up in Petri dishes for subsequent imaging.

A sample location ‘map’ was created to standardize the collection of dicing tape samples. The map was transcribed onto a sheet of butcher paper with 11 sample points distributed in an oval 90 cm wide by 60 cm high (Fig. 8). The sample map was suspended behind the screen (taped to a black cloth used as a photography backdrop) and aligned with the seeding nozzles using reference points on the map and screen. Before and after the initial screen cleaning, dicing tape samples were collected at all the locations on the sample map as well as locations on the screen that appeared particularly fouled. After each wind tunnel test, samples were collected only from the 11 points on the sample map before cleaning the screens.

Dicing tape samples were imaged under a Leica DM8000 M optical microscope using primarily brightfield transmission mode, although reflectance mode (brightfield and darkfield) was used to compare image quality in highly fouled samples. Each dicing tape sample was inspected at low magnification (50x to 200x) to identify the areas of highest PSL density (corresponding to the areas of the screen that were most fouled by PSLs). The areas of high PSL density were imaged at higher magnification, up to 1000x. From each sample, representative images of the two areas of highest PSL density were selected for comparison with other samples from the same set. From each sample set of 11 samples, the image with the highest PSL density was selected to represent the worst-case scenario, for comparison

with other sample sets. Although only one image from each set of 11 samples was used for comparison with other sample sets, roughly 200-500 images were collected for each set, allowing general qualitative comparisons.

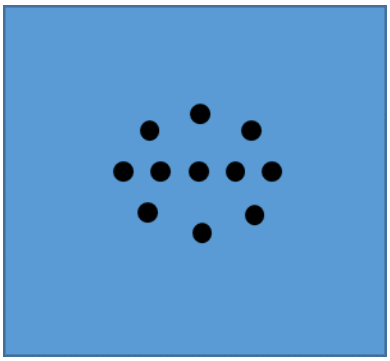

Figure 8. Sample location map for dicing tape samples.

BART PIV Data

PIV data were collected by BART operators using an existing experimental setup. Prior to PSL testing, this setup was tested using the current standard for PIV seeding in BART, a commercial smoke machine (Pea Soup model PS31ST, using Phantom Smoke Oil 135). The smoke machine was supplied with pressurized nitrogen at 100-140 kPa (15-20 psi) and filled the entire room housing BART to ensure even seeding.

Setup/Operation

Equipment

For operation and setup, equipment can be grouped into 4 general categories. Pressurized air lines (1) fed into the nozzles (2) and either the wet seeder (3) or the dry seeder (4). PSLs were pulled from the seeder to the nozzle and expelled into the wind tunnel.

Air Supply

The schematic for pressurized air lines is shown in Figs 9 & 10. House air at 180+ kPa (70+ psi), controlled with a regulator, was used for pressurized air supply. A quick-connect high-pressure hose connected the air supply to a manifold. The manifold had three outlets with 0.64 cm (1/4 in.) high density polyethylene (HDPE) high-pressure tubing (connected by push-to-connect fittings), each connecting to a separate nozzle. The manifold also had one outlet that was fitted with either a plug (for wet seeding) or a hose barb (for dry seeding). No conditioning elements (drying tubes, oil filters, etc.) were used downstream of the diaphragm valve.

Nozzles

The nozzles used for wet and dry seeding operated on different principles but shared some functional similarities. In each system, the nozzle had separate inlets for pressurized air and seed material. The pressurized air inlets were connected directly to the air supply manifold using 0.64 cm (1/4 in.) HDPE tubing and push-to-connect fittings. Nozzle pressure could only be controlled via the regulator at the wall.

Wet seeding used Sonicom SPV2-JDU-HTD ultrasonic nozzles to aerosolize the PSL suspension. PSLs in suspension were delivered to the nozzle under pressure in 0.64 cm (1/4 in.) HDPE tubing.

For dry seeding (Fig. 10), brass spiral cone nozzles designed for wide dispersal of PSLs were mounted on a Venturi vacuum pump (VPs20-100M, Vaccon). Aerosolized particles in the FBS were pulled into the pump through 0.64 (1/4 in.) static-dissipative polyurethane tubing.

Both dry and wet seeding experiments used three nozzles bolted to a movable nozzle mount built from T-slotted extruded aluminum rails (Fig. 11). The frame could be moved to change where in the wind tunnel seed was introduced. Typically, the nozzles were mounted 175 cm above the floor and spaced 15 cm apart horizontally.

Wet Seeder

For wet seeding (Fig. 9), PSL suspension was contained in a pressure vessel (vessels with capacities between 1 and 3 gallons have been used, depending on volume of PSL needed for a test). The vessel was connected to house

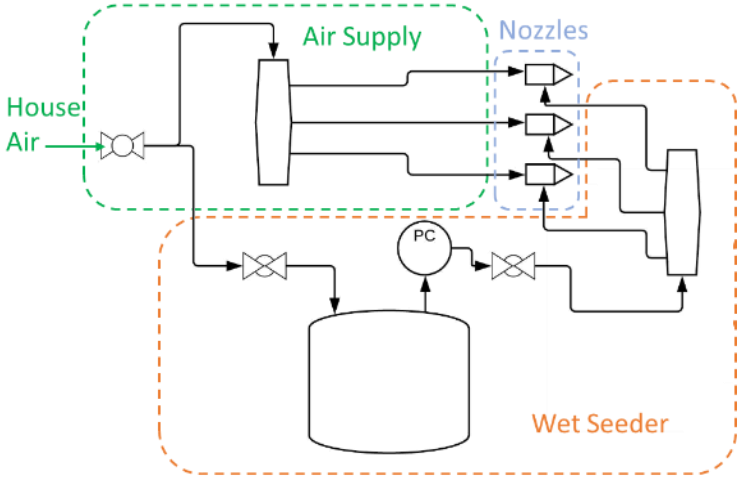

Figure 9. Wet seeder components.

air lines via a quick-connect and ball-valve on the top of the vessel. An outlet line, which drew from the bottom of the vessel, was equipped with a ball valve and regulator to control the flow and pressure of the PSL suspension being fed to the nozzles. A quick-connect fitting connected the regulator to a manifold. The manifold had three outlets, each connected to a nozzle via 0.64 cm (1/4 in.) HDPE tubing. Before each seeding test, a known volume of PSL suspension was poured into the access port on the pressure vessel. After each test the vessel was rinsed with water. The seeder was refilled with water and run for several minutes to flush any PSL suspension remaining in system.

Dry Seeder

Dry seeding was accomplished using a fluidized bed, described earlier (Fig. 10). Air was supplied via 1.3 cm (1/2 in.) reinforced PVC tubing, connected to the manifold via hose barbs. The inlet air flow to the windbox was controlled using a needle valve and monitored using a 0-34.5 kPa (0-5 psi) analog pressure gauge on the windbox. To address concerns about PSL tribocharging in the fluidized bed, a 15.2 cm (6 in.) static eliminator bar (Ion-Edge Model 400T, TAKK Industries) was mounted in the windbox. All metal parts of the fluidized bed were grounded to the grounding pin of the static eliminator bar. Between tests, the fluidized bed was disassembled, cleaned with water, wiped down with lab wipes and thoroughly dried using house air. For a new test, the bed was reassembled, and particles loaded by pouring them into the top. Typically, 10 g of PSLs or blends of PSLs and fumed silica were added to the fluidized bed for each set of particles. The fluidized bed was not broken down and cleaned between tests that used the same type of particles.

Procedures

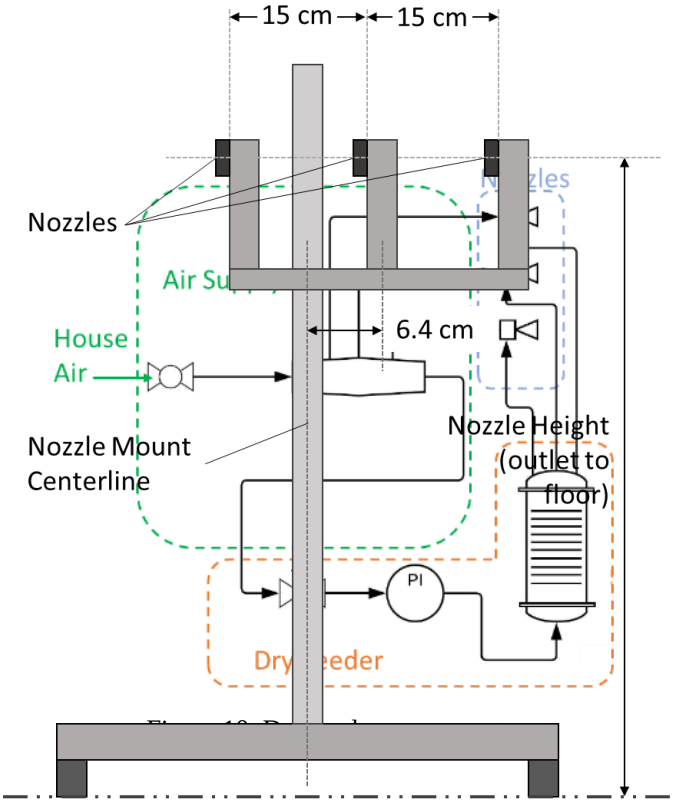

Figure 11. Nozzle mount for PSL seeding

The procedures for BART seeding tests were designed to deal with the limitations presented by the facility and operational requirements. Due to time scheduling constraints, personnel conducting the tests described here were

unable to receive laser safety training before tests commenced and could not be in the same room as the tunnel during PIV data collection. As a result, the flow rate through the fluidized bed could not be changed in response to PIV observations of seed density. Table 2 lists the steps in the process of a given BART test. A total of 12 seeding tests were run in BART (**Appendix C**). Six combinations of operating parameters including seed material, delivery medium, etc. were tested. Each combination was run twice; the first time with the EPC off and the second time with the EPC on. Sampling and cleaning were carried out only after both tests for a given combination of variables were completed.

Table 2. Steps in a BART test

Step	Action	Comments
1	Tunnel flow start-up	All facility doors closed and building ventilation active
2	Wet/Dry seeder startup	Flow to dry seeder slowly increased from zero to operating pressure to prevent blowing PSLs out of reactor during startup
3	All personnel vacate BART room	Overhead lights turned off
4	PIV startup and operation.	
5	System shutdown	Steps 4-3-2-1 in reverse
6	General system observations	
7	Repeat step 1	
8	EPC startup	Voltage slowly increased to target value, verifying that no arcing occurs
9	Repeat steps 2-4	
10	System shutdown	Steps 4-3-2-1 in reverse
11	EPC shutdown	Slowly reduce voltage to zero and verify that no potential remains between electrodes and collector plate
12	Sample collection	EPC plates collected, screen photographed and dicing tape samples collected
13	Clean screen	Using “Shark” steamer
14	Photograph screen to confirm cleaning	
15	Clean lines and nozzles exposed to PSLs	Flush lines, brush nozzles clean

Data Analysis

Two categories of data were collected during the BART testing described here. Screen fouling data were collected from photographs of the screen and microscope images of dicing tape samples. PIV data were captured and analyzed in the usual fashion by BART personnel.

Several factors limited the quantitative comparisons that could be drawn from screen fouling data. The geometry of the screen posed a challenge as it was woven from wires with a round cross section. As a result, there were no flat planes that could be designated as the surface of the screen and each point of overlap between wires resulted in the top wire bulging upwards while the bottom wire was pushed downwards. This, combined with the difficulty of exactly reproducing lighting and camera angles, meant that image analysis of screen photographs would not produce reliable results. However, side-by-side images of the same area of screen were instructive as a general indicator of cleanliness, as will be discussed later. Likewise, it was not feasible to install flat plate witness coupons within the wind tunnel assembly as this was believed to introduce an unnecessary risk to the integrity of the wind tunnel and its constituent parts.

Screen geometry also complicated the analysis of dicing tape samples because the overlapping wires bulged out from the surface of the screen. Dicing tape samples only made contact with the top wire at each overlap and the resulting sample had a cross-hatched pattern of oval spots corresponding to the top wires at each overlap (Fig. 12). As a result, comparison between samples could only be made within the confines of a single spot. For this reason, the spot representing the 'worst-case-scenario' of fouling was found for each sample and used for comparison (as described in data collection methods).

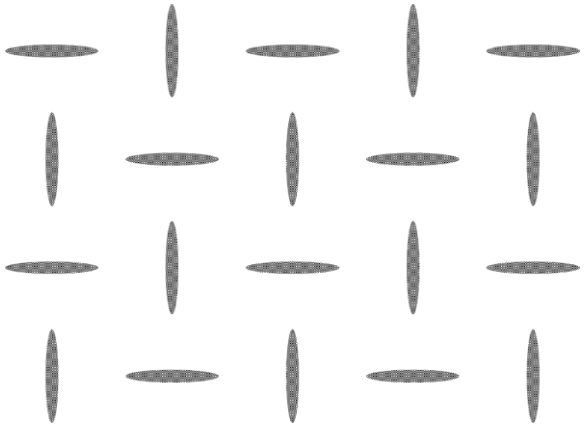

Figure 12. Cross-hatched pattern produced in dicing tape samples due to screen geometry.

Microscope images of dicing tape samples were assessed for three criteria. The total area coverage of particles within a spot was employed as a general measure of extent of fouling. The relative number of single particles compared to aggregates (SP:AG) was an indicator of the ability of a seeding setup to retain and break up aggregates while eluting single particles. The presence of additives (*i.e.*, fumed silica) was also considered, as this could impact PIV measurements and other factors such as necessary health and safety measures.

Results

Screen Fouling

Comparison of the 'worst-case-scenario' samples from each test (Fig. 13) showed marked differences between different types of seeding. PSLs wet-seeded from 1:1 water:ethanol appeared to produce the most fouled screens, with a thick and uniform covering of particles on dicing tape samples. The coating of PSLs was so thick that it was impossible to estimate total area coverage because the particles formed a nearly continuous particle coating. Wet seeding from ethanol showed the second highest area coverage of all tests, although particle coverage was visibly less than for the 1:1 case. Both wet seeding cases resulted in considerable amounts of PSL aggregates on the screen. The number and size of aggregates could not be easily estimated because many of the aggregates were flattened when the dicing tape was pressed onto the screens, but it appeared that most of the particles observed on the dicing tape were originally present on the screen in aggregates. Most of the aggregates for the ethanol sample were of a similar size, composed of 10-50 PSLs. The low SP:AG ratio on screen samples is worth noting because previous work by

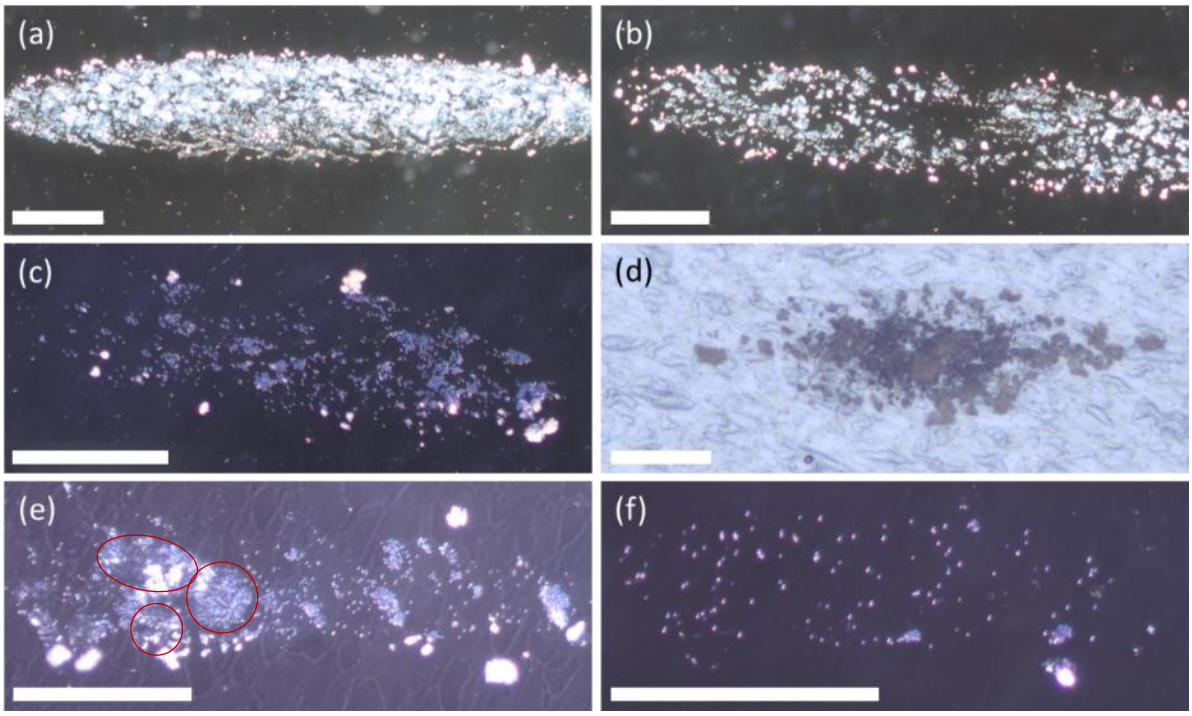

Figure 13. Microscope images of "worst-case scenarios" for each particle type and seeding media. A) uPSLs in water/ethanol, B) uPSLs in ethanol, C) uPSLs dry, D) uPSLs dry and blended with fumed silica, E) fPSL 10-10-DAB dry and F) fPSL CTAB dry. Note the fumed silica contamination in E (circled in red). All scale bars are 100 micrometers.

NASA researchers (only described through word of mouth) was based on the assumption that wet seeding produced only single particles, an assumption disproved by these results.

Dry seeding samples showed less fouling than wet seeding. Dry seeding uPSLs with fumed silica additive resulted in large amounts of fumed silica present on screens and samples of dry-seeded fPSL-10-10-DAB, which was tested directly after the fumed silica mixture, also showed contamination by fumed silica. The source of the fumed silica in these samples is assumed to be fumed silica that remained in the seeding tubing from the previous test. The presence of fumed silica on dicing tape samples made imaging of the PSLs difficult but overall the area coverage of dry seeded uPSL, uPSL with fumed silica and fPSL 10-10-DAB appeared comparable. Aggregates were observed in dry seeded samples but the SP:AG ratio was observed to be higher in all dry seeding tests compared to wet seeding. Conclusions about the size distribution of aggregates could not be reached based on limited information. Samples from dry-seeded fPSL CTAB were clearly less fouled than those from any other tests and showed the highest SP:AG ratio of any test. Photographs of the screen could not resolve individual particles but appeared to confirm the trends observed in dicing tape samples and the presence of aggregates in all cases (Fig. 14).

Quantitative data on total particles seeded was not available for these tests; therefore, it was impossible to say that the screens were exposed to the same, or even to similar, amounts of particles during each run. However, comparisons can be made between the quality of PIV data obtained and the level of particle fouling. For example, the uPSL/silica mixture and fPSL CTAB both gave a very similar quality of PIV data, but fPSL CTAB produced significantly less screen fouling (Fig. 13).

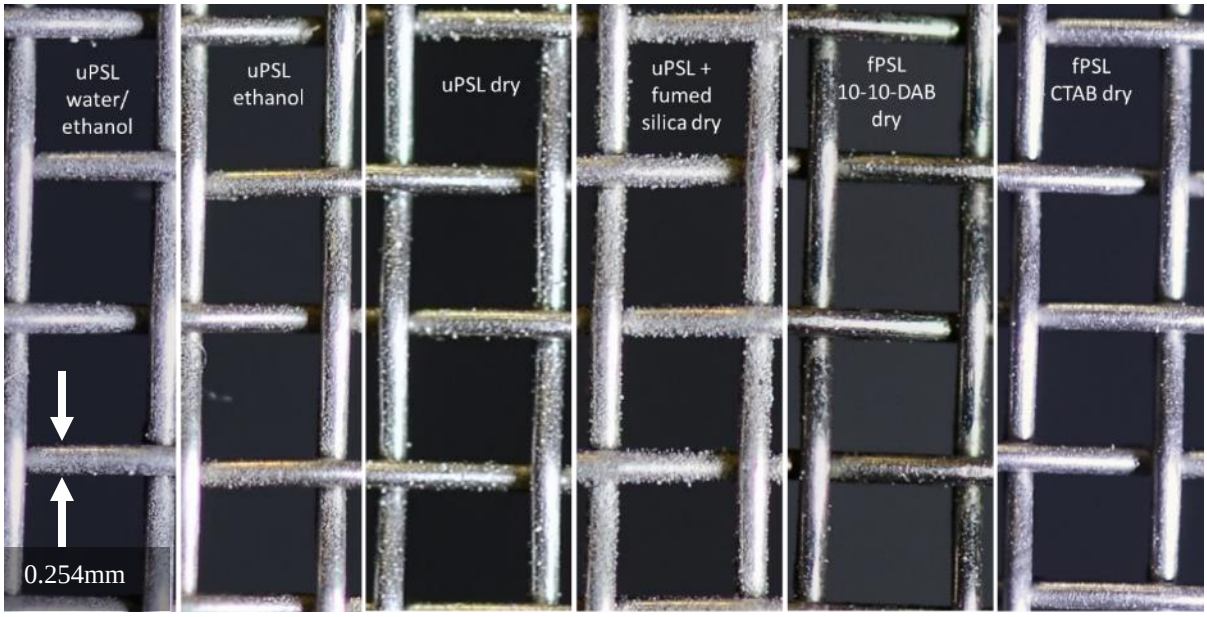

Figure 14. Photographs of the same screen location after each seeding test.

BART PIV Data

Two pieces of PIV data were obtained from tests in BART; a vector map of the measured flow velocities (U) over the wing test section, and a ΔU map showing the difference in measured velocities between the current seeding method and the smoke seeding baseline previously obtained (Fig. 15). Figure 15 shows the velocity map baseline generated using a smoke machine. Figure 16 shows the ΔU maps from each seeding method. The ΔU maps are generated using the second set of PIV data from each sample condition with the exception of the dry uPSL data, where only one set of

PIV data was captured. For each sample condition, the second set of PIV data shows better agreement with the smoke machine data because the seeder operating conditions were refined between the first and second runs based on observations from the first run. The first PSL seeding test conducted was with dry uPSL and included much of the initial troubleshooting and tuning for the dry seeding setup. This troubleshooting and the lack of a second PIV data set likely contributed to the poor ΔU agreement in the dry uPSL run compared to later runs.

ΔU maps show that dry seeding of PSLs was able to generate accurate PIV data across most of the test section. All dry seeding tests had difficulty with resolving flow within the more complex turbulent boundary layer of the wing model. Smoke seeding and traditional wet seeding methods were able to resolve flow field properties to approximately the same level of resolution. The limited resolution for PIV data generated with dry seeding was due to low seeding density in the area of interest when using the fluidized bed. The seeding density in the area of interest

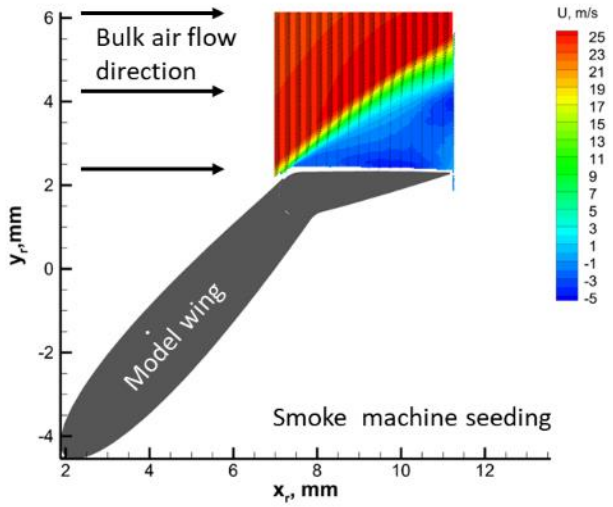

Figure 15. Velocity (U) data using smoke machine for seeding.

was affected by the overall single particle flux out of the bed as well as the location of the seeding nozzles relative to the model.

Improvements were seen between dry seeding tests when the pressure through the bed increased, thus seeding more particles into the flow. Quantitative comparison of particle counts seeded across various tests was not possible at the time of testing.

Of particular note is that tests with dry fPSLs and the uPSL/fumed silica mixture produced PIV data that were very close to the wet seeded PSLs, with the exception of the thin boundary layer at the wing flap surface.

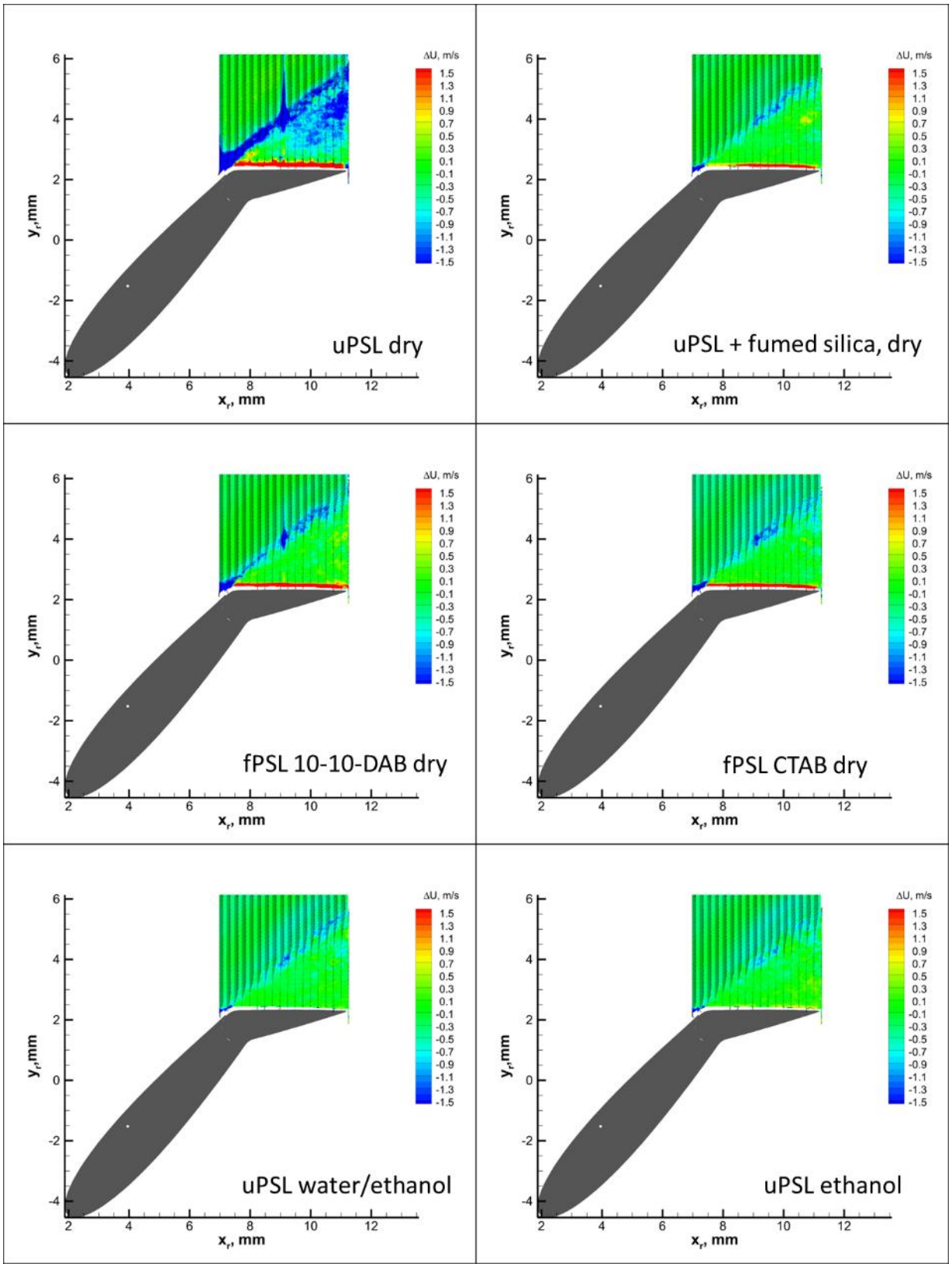

Figure 16. ΔU maps for various seeding conditions.

Future Work

Tests at BART indicate that dry seeding of PSLs into wind tunnels has potential for obtaining PIV data comparable with traditional wet seeding methods while reducing screen fouling. Improvements to seeding density from dry formulations are desired and would allow dry seeding to produce data of equal quality to wet seeding. Changes in nozzle design, fluidized bed dimensions, and other techniques to better control the distribution of seeded airflow once the PSLs have been aerosolized may improve the seed density and distribution within the analytical space of a PIV experiment.

Improvements to the dry seeding methods may be made through modifications to the surface composition of the particles or the seeding equipment. Tests with fumed silica additives in a fluidized bed found that fumed silica did improve fluidization quality but also dramatically increased screen fouling. Therefore, adding fumed silica to the fluidized bed is not a viable method to improve dry PSL seeding. Other approaches to improve fluidization that do not adversely impact surface contamination may yield greater PSL airflow seed densities, and are discussed below.

Differences in screen fouling were observed between modified and unmodified PSLs used in dry seeding. The fPSL tests all resulted in less screen fouling than the uPSL tests, while PIV data quality was comparable. More studies are required to clarify the relationship between PSL modification and screen fouling, but these initial results indicate that PSL modification is a viable method to decrease screen fouling in wind tunnels.

Modifications to Instrumentation

The tests described in this document facilitated qualitative comparisons of different seeding methods and materials; yet, quantitative comparisons could not be made. The control system of the fluidized bed did not allow sufficiently fine control or measurement of flow through the bed, meaning that substantial differences in flow rate may have existed between different dry seeding runs. As noted, the Venturi nozzles pulled air out of the FBS and the screened make-up air/excess air port at the top of the bed allowed the bed to operate at positive or negative pressure. Since only the pressure in the windbox was measured, the relative flow rate into the bed could not be calculated and it was observed that even large changes in flow rate (as the inlet valve was opened and flow through the bed could be seen to increase the movement of particles) had a small effect on the pressure in the windbox. Therefore, a given pressure reading could correspond to a wide range of flow rates. To remedy this, a flowmeter should be introduced between the needle valve and the windbox.

Pressurized air was supplied to the FBS and the nozzles through the same manifold, which, in turn, was delivered by a hose. The flow of pressurized air to the nozzles determined the vacuum applied by the nozzles to the FBS; the only method to control flow was to adjust the pressure into the pressurized hose that fed the manifold. It may be expected that increasing flow to the FBS would thus decrease flow to the nozzles, thereby decreasing the pull of the nozzles from the FBS. Unfortunately, no control elements allowed measurement of flow to the nozzles, the manifold or the FBS. Therefore, it is unknown how much, if any, variation in nozzle flow rate existed between tests. This could be addressed by supplying the nozzles and FBS from independent pressurized air sources and/or introducing flow measure and control elements into the lines feeding the nozzles and fluidized bed.

Wet seeding produced higher seed density in PIV measurements compared to dry seeding, but also resulted in higher PSL fouling of the screen. The fraction of particles seeded that were deposited on the screen is an important parameter for comparing the utility of a given seeding method and material. In the BART tests described in this document, the measurement of the total number of particles seeded was not available. Therefore, the relative likelihood of a particle sticking to the screen could not be compared between methods and it could not be definitively shown that dry seeding would produce less fouling for the same PIV seed density compared to wet seeding. It is reasonable to expect, however, that aggregates, having higher momentum than single particles, would be more likely to exit the air flow and impact on screens. Therefore, the effect of seed size distribution (single particles or aggregates)

on screen fouling could not be clearly determined. This could be addressed by introducing a particle counter into the wind tunnel during operation. Measuring the total number of particles entrained in flow and measuring the size distribution of the particles would allow quantitative comparisons between techniques to determine the fraction of seeded particles adhering to the screen and the total number and quality of particles seeded at various conditions.

Modifications to the Fluidized Bed Seeder

As discussed in the design of the FBS, a critical requirement for the FBS involves the ability to break up PSL aggregates into single particles and to retain the aggregates while seeding only single particles.

Retaining Particles

Considering the small size of PSLs and their propensity for clumping, the use of in-line filters to retain aggregates while passing single particles was deemed impractical. This was confirmed by preliminary testing with various filter materials. An attractive alternative is the separation of particles based on mass. The simplest way to do this is to increase the height of the FBS riser, which increases the distance over which a particle must remain entrained in the air flow before it can be eluted. Since the larger particles are less readily entrained in flow, the likelihood that they will not be eluted increases with the height of the riser, analogous to a chromatography column.

A common industrial and commercial method for separating particles from airflow is cyclonic separation, where particles are separated based on their momentum (and therefore mass). In a cyclonic separator, a stream of fluid with entrained particles is directed into a column so that a vortex forms. For particles entrained in flow, the larger the momentum of a particle the longer it takes for the particle to respond to changes in fluid velocity. Therefore, larger particles do not follow the curve of the rotational flow in a vortex as well as smaller ones and are more likely to impact the wall of the column and fall to a lower part of the riser. The concepts of fluidized beds and cyclone separation can be combined by introducing a vortex in the riser of the fluidized bed or in the fluidized bed itself. A common application of such "vortexing fluidized beds" is in combustors, as a method to increase combustion efficiency and reduce emission of pollutants[56–59]. In the same way, introducing a vortex in the FBS riser could improve the retention of aggregates while allowing single particles to elute. A vortex may be induced in the riser or bed by using secondary (horizontal) jets of air or by replacing the distributor with an array of small nozzles that introduces a vortex in the bed and air above it[56].

Breaking Up Aggregates/Deagglomeration

Fine particles are prone to agglomeration in the dry state due to interparticle forces such as van der Waals and electrostatic interactions. Agglomeration does, however, depend on the particles being close enough to interact with one another. Therefore, agglomeration may be unavoidable in a fluidized bed but not a concern for particles already eluted from the bed. In a fluidized bed, agglomeration and deagglomeration are expected to approach a dynamic equilibrium, where the rate of agglomerate break-up into single particles matches the rate of single particle agglomeration[48,60]. If individual particles are preferentially removed, deagglomeration would be favored as the system equilibrates. If agglomeration is insignificant once particles leave the fluidized bed, the net result of the competing processes in the bed is continual production of single particles from agglomerates. As a convenient result, PSL agglomeration does not need to be completely prevented to, eventually, elute most of the PSLs as single particles. From an application standpoint, the maximum flux of single particles out of the FBS is limited by the rate of single particle production in the bed and therefore the rate of deagglomeration.

Increasing the rate of deagglomeration within the FBS may be desired to increase the rate of PSL seeding. The phenomena behind deagglomeration are relevant to applications including production of alloys, powder coating or impregnation and drug delivery systems[60]. Existing methods to drive deagglomeration include mechanical

impaction or vibration, acoustic pressure, and introduction of turbulence[61]. For application to the system described here, inspiration may be taken from the design of pharmaceutical dry powder inhalers (DPIs), which share many features with the FBS. Both systems are charged with aggregation-prone micrometer-scale particles that must be deagglomerated and eluted as an aerosol with a uniform particle size distribution. In the case of DPIs, control of eluted particle size is required to create an aerosol that will travel deep into the lungs before depositing[37,61].

As discussed above, a vortex may be introduced to the bed via modifications to the distributor. Introducing a vortex may be used to increase retention of large particles but it can also increase turbulence within the bed, introducing a horizontal component to the flow, allowing greater maximum fluid velocity and increasing shear within the bed. The potential to simultaneously increase agglomerate retention and the rate of deagglomeration makes a vortexing fluidized bed an attractive option for FBS modification.

Modification of PSLs

Chemical modification of PSL surfaces with quaternary ammonium surfactants is being investigated as a method to improve PSL properties for use in the fluidized bed seeder and in wind tunnels. As mentioned previously, unmodified PSLs contain acid surface groups that impart hydrophilic properties on the particles. Reports in the literature suggest that modification of PSLs with QAs can reduce the hydrophilicity of PSLs and the polar component of the PSL interfacial energy[62,63]. Future work for PSL modification includes varying the length and number of alkyl chains on QAs and identifying optimal QA loading for dry seeding performance.

Conclusion

Testing at BART successfully demonstrated the potential for PSLs to be seeded as wind tunnel tracers from the dry state. PIV data generated from these tests showed agreement with the current seeding methods and identifying areas for further development. The tests also laid the foundation for future investigations of novel seeding methods in an active research wind tunnel, establishing methods for seeder deployment, data collection and data analysis. Future work on dry seeding PSLs includes chemical modification of PSLs, modified instrumentation for improved system characterization and methods to increase dry seed density from a fluidized bed seeder.

References

1. Nichols, C. *NASA-TM-89163: Preparation of Polystyrene Microspheres for Laser Velocimetry in Wind Tunnels*. (1987).
2. Wohl, C. J., Tiemsin, P. I., Robbins, S. J. & Page, A. *NASA-TM-2018-219835: Mitigation of Polystyrene Microsphere Surface Contamination for Wind Tunnel Applications*. (2018).
3. Li, Z. *et al.* Novel Wire-on-Plate Electrostatic Precipitator (WOP-EP) for Controlling Fine Particle and Nanoparticle Pollution. *Environ. Sci. Technol.* **49,** 8683–8690 (2015).
4. Kotera, A., Furusawa, K. & Takeda, Y. Colloid chemical studies of polystyrene latices polymerized without any surfaceactive agents - I. Method for preparing monodisperse latices and their characterization. *Kolloid-Zeitschrift Zeitschrift fur Polym.* **239,** 677–681 (1970).
5. Stone-Masui, J. & Watillon, A. Characterization of surface charge on polystyrene latices. *J. Colloid Interface Sci.* **52,** 479–503 (1975).
6. Tauer, K., Deckwer, R., Kühn, I. & Schellenberg, C. A comprehensive experimental study of surfactant-free

emulsion polymerization of styrene. *Colloid Polym. Sci.* **277,** 607–626 (1999).
7. Goodwin, J., Hearn, J., Ho, C. & Ottewill, R. Studies on the preparation and characterisation of monodisperse polystyrene latices .3. Preparation without added surface active agents. *Colloid Polym. Sci.* **252,** 464–471 (1974).
8. Chern, C. S., Lin, S. Y. & Hsu, T. J. Effects of Temperature on Styrene Emulsion Polymerization Kinetics. **31,** 516–523 (1999).
9. Dobrowolska, M. E., Van Esch, J. H. & Koper, G. J. M. Direct visualization of 'coagulative nucleation' in surfactant-free emulsion polymerization. *Langmuir* **29,** 11724–11729 (2013).
10. Kuehn, I. & Tauer, K. Nucleation in Emulsion Polymerization: A New Experimental Study. 1. Surfactant-Free Emulsion Polymerization of Styrene. *Macromolecules* **28,** 8122–8128 (1995).
11. Antonietti, M. & Tauer, K. 90 Years of polymer latexes and heterophase polymerization: More vital than ever. *Macromol. Chem. Phys.* **204,** 207–219 (2003).
12. Madaeni, S. S. & Ghanbarian, M. Characterization of polystyrene latexes. *Polym. Int.* **49,** 1356–1364 (2000).
13. Vanderhoff, J. W. Mechanism of emulsion polymerization. *J. Polym. Sci. Polym. Symp.* **198,** 161–198 (1985).
14. Ugelstad, J., El-Aasser, M. S. & Vanderhoff, J. W. Emulsion polymerization: initiation of polymerization in monomer droplets. *J. Polym. Sci. Polym. Lett. Ed.* **11,** 503–513 (1973).
15. Ngai, T. & Wu, C. Double roles of stabilization and destabilization of initiator potassium persulfate in surfactant-free emulsion polymerization of styrene under microwave irradiation. *Langmuir* **21,** 8520–8525 (2005).
16. Schork, F. J. *et al.* Miniemulsion polymerization. *Adv. Polym. Sci.* **175,** 129–255 (2005).
17. Tauer, K. & Hernandez, H. Mechanism and Modeling of Emulsion Polymerization: New Ideas and Concepts-2. Modeling Strategies. *Macromol. Symp.* **288,** 9–15 (2010).
18. Hearn, J., Wilkinson, M. C., Goodall, A. R. & Chainey, M. Kinetics of the Emulsion Polymerization of Styrene. *J. Am. Chem. Soc.* **67,** 1674–1680 (1985).
19. Chern, C. S. Emulsion polymerization mechanisms and kinetics. *Prog. Polym. Sci.* **31,** 443–486 (2006).
20. Furusawa, K., Norde, W. & Lyklema, J. A method for preparing surfactant-free polystyrene latices of high surface charge. *Kolloid-Zeitschrift Zeitschrift fur Polym.* **250,** 908–909 (1972).
21. Goodwin, J. W., Hearn, J., Ho, C. C. & Ottewill, R. H. The Preparation and Characterisation of Polymer Latices Formed in the Absence of Surface Active Agents ". *Br. Polym. J.* **5,** 347–362 (1973).
22. Telford, A. M., Pham, B. T. T., Neto, C. & Hawkett, B. S. Micron-sized polystyrene particles by surfactant-free emulsion polymerization in air: Synthesis and mechanism. *J. Polym. Sci. Part A Polym. Chem.* **51,** 3997–4002 (2013).
23. Ottewill, R. H. & Shaw, J. N. Studies on the Preparation and Characterisation of Monodisperse Polystyrene Latices Part 2: Electrophoretic Characterisation of Surface Groupings. *Kolloid-Zeitschrift Zeitschrift fur Polym.* 34–40 (1966).
24. Brouwer, W. M. & Zsom, R. L. J. Polystyrene latex particle surface characteristics. *Colloids and Surfaces* **24,** 195–208 (1987).
25. Siqueira-Petri, D. F. *et al.* Surface modification of thin polystyrene films. *Colloid Polym. Sci.* **277,** 673–679 (1999).
26. Smith, J. A. & Galan, A. Sorption of Nonionic organic Contaminants to Single and Dual Organic Cation Bentonites from Water. *Enviromental Sci. Technol.* **29,** 685–692 (1995).
27. Shimizu, M., Saito, T., Fukuzumi, H. & Isogai, A. Hydrophobic, ductile, and transparent nanocellulose films with quaternary alkylammonium carboxylates on nanofibril surfaces. *Biomacromolecules* **15,** 4320–4325 (2014).
28. Xhanari, K., Syverud, K., Chinga-Carrasco, G., Paso, K. & Stenius, P. Reduction of water wettability of nanofibrillated cellulose by adsorption of cationic surfactants. *Cellulose* **18,** 257–270 (2011).
29. Notley, S. M. Direct visualization of cationic surfactant aggregates at a cellulose-water interface. *J. Phys.*

Chem. B **113,** 13895–13897 (2009).
30. Rosen, M. J. Micelle Formation by Surfactants. *Surfactants Interfacial Phenom.* 105–177 (2004). doi:10.1002/0471670561.ch3
31. Geldart, D. Types of gas fluidization. *Powder Technol.* **7,** 285–292 (1973).
32. Chalovich, J. M. & Eisenberg, E. NIH Public Access. *Biophys. Chem.* **257,** 2432–2437 (2012).
33. Zahedi, K. & Melcher, J. R. Collection of Submicron Particles in Bubbling Electrofluidized Beds. *Ind. Eng. Fundam.* **16,** 248–254 (1977).
34. Kaliyaperumal, S., Barghi, S., Zhu, J., Briens, L. & Rohani, S. Effects of acoustic vibration on nano and sub-micron powders fluidization. *Powder Technol.* **210,** 143–149 (2011).
35. Sahoo, P. External Force and vis-à-vis comparison against Fine Particle Fluidization. in *2013 International Conference on Energy Efficient Technologies for Sustainability* 853–858 (2013).
36. Bruni, G., Colafigli, A., Lettieri, P. & Elson, T. Torque Measurements in Aerated Powders Using a Mechanically Stirred Fluidized Bed Rheometer (msFBR). *Chem. Eng. Res. Des.* **83,** 1311–1318 (2005).
37. Newman, S. P. & Busse, W. W. Evolution of dry powder inhaler design, formulation, and performance. *Respir. Med.* **96,** 293–304 (2002).
38. Bouillard, J. X. & Gidaspow, D. On the Origin of Bubbles and Geldart Classification. *Powder Technol.* **68,** 13–22 (1991).
39. Langde, A. M., Tidke, D. J. & Sonolikar, R. L. Experimental investigation of minimum fluidization velocity of micron size particles in presence of sound. *Int. Conf. Emerg. Trends Eng. Technol. ICETET* 207–210 (2012). doi:10.1109/ICETET.2012.58
40. Brekken, R. A. Gas fluidization of wheat flour in a stirred bed. (Iowa State University, 1968).
41. Celeste, B. M. Celeste , Brian M . The Combined Effects of Mechanical and Acoustic Vibrations on a Fluidized Bed of Geldart C Particles September 2004. (Lehigh University, 2004).
42. Kuipers, N., Stamhuis, E. & Beenackers, A. Fluidization of potato starch in a stirred vibrating fluidized bed. *Chem. Eng. Sci.* **51,** 2727–2732 (1996).
43. Tomasetta, I., Barletta, D., Lettieri, P. & Poletto, M. The measurement of powder flow properties with a mechanically stirred aerated bed. *Chem. Eng. Sci.* **69,** 373–381 (2012).
44. Levy, E. K. & Celeste, B. Combined effects of mechanical and acoustic vibrations on fluidization of cohesive powders. *Powder Technol.* **163,** 41–50 (2006).
45. Wang, Z., Kwauk, M. & Li, H. Fluidization of fine particles. *Chem. Eng. Sci.* **53,** 377–395 (1998).
46. Morooka, S., Kusakabe, K., Kobata, A. & Kato, Y. Fluidization state of ultrafine powders. *J. Chem. Eng. Japan* **21,** 41–46 (1988).
47. Chan, A. T. & Lewis, J. A. Size Ratio Effects on Interparticle Interactions and Phase Behavior of Microsphere - Nanoparticle Mixtures. *Langmuir* **24,** 11399–11405 (2008).
48. Hakim, L. F., Portman, J. L., Casper, M. D. & Weimer, A. W. Aggregation behavior of nanoparticles in fluidized beds. *Powder Technol.* **160,** 149–160 (2005).
49. Kraus, M. N. Pneumatic Conveying Systems. *Chem. Eng.* **93,** 50–61 (1986).
50. Melling, A. Tracer particles and seeding for particle image velocimetry. *Meas. Sci. Technol.* **8,** 1406–1416 (1997).
51. Chen, Y., Yang, J., Dave, R. & Pfeffer, R. Fluidization of coated group C powders. *IFAC Proc. Vol.* **7,** 405–410 (2009).
52. Murtomaa, M. *et al.* Electrostatic measurements on a miniaturized fluidized bed. *J. Electrostat.* **57,** 91–106 (2003).
53. Zhang, W., Yan, Y., Qian, X., Guan, Y. & Zhang, K. Measurement of Charge Distributions in a Bubbling Fluidized Bed Using Wire-Mesh Electrostatic Sensors. *IEEE Trans. Instrum. Meas.* **66,** 522–534 (2017).
54. Park, A. H., Bi, H. & Grace, J. R. Reduction of electrostatic charges in gas-solid fluidized beds. *Chem. Eng. Sci.* **57,** 153–162 (2002).

55. Chaouki, J., Chavarie, C., Klvana, D. & Pajonk, G. Effect of interparticle forces on the hydrodynamic behaviour of fluidized aerogels. *Powder Technol.* **43,** 117–125 (1985).
56. De Wilde, J. Gas-solid fluidized beds in vortex chambers. *Chem. Eng. Process. Process Intensif.* **85,** 256–290 (2014).
57. Dvornikov, N. A. Combustion in vortex chambers with a fluidized particle bed. *Combust. Explos. Shock Waves* **51,** 631–640 (2015).
58. Sathitruangsak, P., Madhiyanon, T. & Soponronnarit, S. Rice husk co-firing with coal in a short-combustion-chamber fluidized-bed combustor (SFBC). *Fuel* **88,** 1394–1402 (2009).
59. Pitsukha, E. A., Teplitskii, Y. S. & Borodulya, V. A. Entrainment of Solid Particles from a Fluidized-Bed Cyclone Chamber. *J. Eng. Phys. Thermophys.* **89,** 1087–1092 (2016).
60. Weiler, C., Wolkenhauer, M., Trunk, M. & Langguth, P. New model describing the total dispersion of dry powder agglomerates. *Powder Technol.* **203,** 248–253 (2010).
61. Voss, A. & Finlay, W. H. Deagglomeration of dry powder pharmaceutical aerosols. *Int. J. Pharm.* **248,** 39–50 (2002).
62. Ganachaud, F. *et al.* Surface characterisation of amine-containing latexes by charge titration and contact angle measurements. *Colloids Surfaces A Physicochem. Eng. Asp.* **137,** 141–154 (1998).
63. Zhao, J. X. & Brown, W. Adsorption of alkyltrimethylammonium bromides on negatively charged polystyrene latex particles using dynamic light scattering and adsorption isotherm measurements. *Langmuir* **11,** 2944–2950 (1995).

Appendix A: Surfactant-Free Emulsion Polymerization

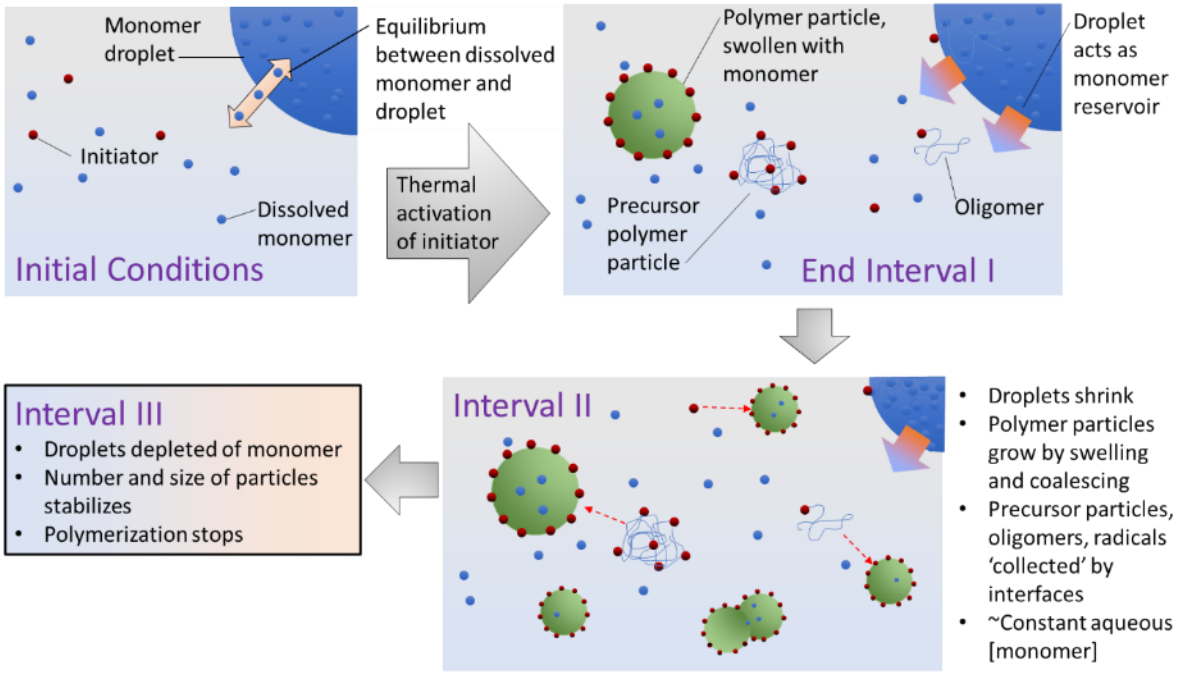

Figure A17. Mechanisms of SFEP.

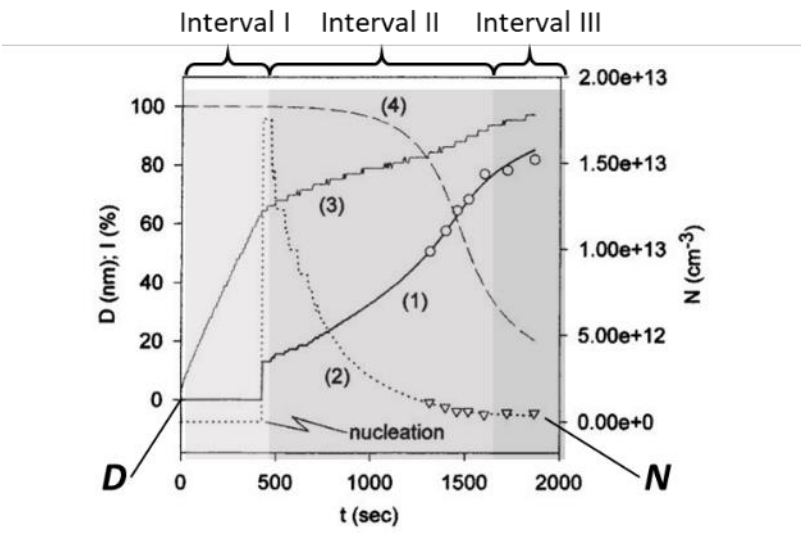

Figure A18. The intervals of SFEP. Adapted from Tauer, 1999. "On-line determination of average particle size and particle number in surfactant-free emulsion polymerization of styrene (recipe A). *1* - average particle size (D); *open circles*: off-line particle size from dynamic light scattering. *2* - particle number (N); *open triangles*: off-line particle numbers. *3* - conductivity (no y-axis). *4* - optical transmission (I).

Table A3. Base recipe for SFEP

Chemical	Mass (g)	Initial Solution Concentration (mM)
Water	2000	-
Styrene	200	-
MgSO4	0.25	1
KPS	1.61	3

Appendix B: PSL Functionalization

$$\left(\frac{100\ cm^3 particles}{liter\ \text{PSL}}\right) * \frac{\left(\frac{area}{particle}\right)}{\left(\frac{volume}{particle}\right)} * \frac{\left(\frac{1\ \text{QA}\ molecule}{2nm^2}\right)}{\left(\frac{6.022x10^{23} molecules}{mol}\right)} = 5\ x10^{-4}\ \frac{mol\ \text{QA}}{liter\ \text{PSL}} \quad \text{(Eq.1)}$$

$$\frac{\left(\frac{area}{particle}\right)}{\left(\frac{volume}{particle}\right)} = \frac{\pi D^2}{\left(\frac{\pi D^3}{6}\right)} = \frac{6}{D} \quad \text{(Eq.2)}$$

Table B1. Critical Micelle Concentrations of QAs

Quaternary Alkylammonium	Critical Micelle Concentration (mM)	Addition 1 (mg)	Addition 2 (mg)	Final Concentration (mM)
Didodecyldimethyl Ammonium Bromide (10-10-DAB)	1.9 (25 °C)	302	309	1.5
Cetyltrimethyl Ammonium Bromide (CTAB)	1.3 (30 °C)	264	101	1

Appendix C: BART Testing Data Collection

Table C1. Dry seeding tests in BART

Case	Particle Type	Date	Pressure at Wall (PSIG)	Pressure at Bed (PSIG)	Nozzle Offset (Inches)	Start Time	Stop Time	Notes
Case 0	UPSL, 022908	3/21/17	23	0.1	0	Not Recorded	Not Recorded	Ion Bar on
Case 1	UPSL, 022908	3/21/17	30	0.3	0	Not Recorded	Not Recorded	
Case 2	PSL + SiO, 030608	3/22/17	30	0.1	16	9:59am	10:11am	Ion bar on, violent bubbling
Case 3	PSL + SiO, 030608	3/22/17	30	0.1	16	10:23am	10:34am	Ion bar on
Case 4	FPSL – 10, 030907	3/22/17	35	0.1	16	1:21pm	1:30pm	
Case 5	FPSL – 10, 030907	3/22/17	40	0.3	16	1:50pm	2:01pm	Valve at bed fully open
Case 6	FPSL – 14, 030907	3/23/17	40	0.2	16	9:46am	9:59am	Well fluidized, flakey particles
Case 7	FPSL – 14, 030907	3/23/17	60	0.5	16	10:15am	10:26am	Valve at bed fully open

Table C2. Wet seeding tests in BART (note that Case 8 is not reported because it was aborted without collecting data)

Case	Particle Type	Date	Nozzle Pressure (PSIG)	Tank Pressure (PSIG)	Nozzle Offset (Inches)	Start Time	Stop Time	Notes
Case 9	PSLs in ethanol, 022008	3/24/17	70	13	16	9:40am	9:50am	Particles depleted at end of run
Case 10	PSLs in ethanol, 022008	3/24/17	70	13	16	10:01am	10:14am	Particles depleted at end of run
Case 11	PSLs in 1:1 water:ethanol. 030608	3/24/17	70	13	16	10:58am	11:07am	Particles depleted at end of run
Case 12	PSLs in 1:1 water:ethanol. 030608	3/24/17	70	13	16	11:27am	11:32am	Particles depleted at end of run

Fluidized Bed Operation Log
BART Testing

Date	
Particle Batch ID	
Sample Name/Run name	

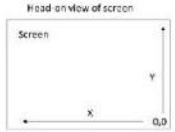

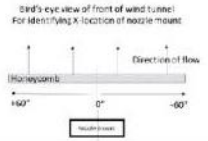

	Pressure at Wall (PSIG)	Mean Pressure at Bed (PSIG)	Nozzle Height (inches)	Nozzle mount X offset (inches)	Tunnel Wind Speed in Test Section (m/s)	Start Time	Stop Time	Notes
Seeding interval 1								
Seeding interval 2								
	X,Y center of sample area	X,Y center of contact paper	X,Y center of Photos	PSL jar initial wieght	PSL Jar final weight	Nozzle Initial weight	Weight of PSLs plus nozzle recovered from FB	
Sample Collection 1								
Sample Collection 2								

Figure C1. Data collection form for BART tests

REPORT DOCUMENTATION PAGE

Form Approved
OMB No. 0704-0188

1. REPORT DATE *(DD-MM-YYYY)*
1-04-2019

2. REPORT TYPE
Technical Memorandum

3. DATES COVERED *(From - To)*

4. TITLE AND SUBTITLE

Reduction of Wind Tunnel Contamination During Flow Visualization Experiments using Polystyrene Microspheres

5a. CONTRACT NUMBER

5b. GRANT NUMBER

5c. PROGRAM ELEMENT NUMBER

6. AUTHOR(S)

Schmitz, Russell C.; Genzer, Jan; Tiemsin, Pacita I.; Whol, Christopher J.

5d. PROJECT NUMBER

5e. TASK NUMBER

5f. WORK UNIT NUMBER
147016.03.07.01.11.02

7. PERFORMING ORGANIZATION NAME(S) AND ADDRESS(ES)

NASA Langley Research Center
Hampton, VA 23681-2199

8. PERFORMING ORGANIZATION REPORT NUMBER
L-20985

9. SPONSORING/MONITORING AGENCY NAME(S) AND ADDRESS(ES)

National Aeronautics and Space Administration
Washington, DC 20546-0001

10. SPONSOR/MONITOR'S ACRONYM(S)
NASA

11. SPONSOR/MONITOR'S REPORT NUMBER(S)
NASA-TM-2019-220245

12. DISTRIBUTION/AVAILABILITY STATEMENT

Unclassified-
Subject Category 23
Availability: NASA STI Program (757) 864-9658

13. SUPPLEMENTARY NOTES

14. ABSTRACT

Evaluation of novel methods and materials for seeding tracer particles for particle image velocimetry (PIV) was carried out in the Basic Aerodynamic Research Tunnel (BART) at NASA's Langley Research Center (LaRC). Seeding of polystyrene latex microspheres (PSLs) from ethanol/water suspensions and from the dry state was carried out using custom built seeders. PIV data generated using the novel methods were found to be in general agreement with data collected using the current seeding methods. Techniques for assessing PSL fouling of wind tunnel surfaces were identified and refined. Initial results suggest that dry seeding PSLs may allow comparable data quality to wet seeding while reducing wind tunnel screen fouling. Results also indicate that further developments to the dry seeding system should focus on increasing single particle flux into the wind tunnel. Modifications to PSLs and seeding equipment to achieve this have been identified and are discussed.

15. SUBJECT TERMS

Adhesion; Contamination; Particle Image Velocimetry; Seeded Airflow

16. SECURITY CLASSIFICATION OF:			17. LIMITATION OF ABSTRACT	18. NUMBER OF PAGES	19a. NAME OF RESPONSIBLE PERSON
a. REPORT	b. ABSTRACT	c. THIS PAGE			STI Help Desk (email: help@sti.nasa.gov)
U	U	U	UU	43	19b. TELEPHONE NUMBER *(Include area code)* (757) 864-9658